Influence of three-Way catalyst on gaseous and particulate matter emissions during gasoline direct injection engine cold-start

Bogarra Macias, Maria; Herreros, Jose; Hergueta Santos-Olmo, Cruz; Tsolakis, Athanasios; York, Andrew ; Millington, Paul

DOI:
10.1595/205651317x696315

http://dx.doi.org/10.1595/205651317X696315 *Johnson Matthey Technol. Rev.*, 2017, **61**, (4), 329–341

JOHNSON MATTHEY
TECHNOLOGY REVIEW
www.technology.matthey.com

Influence of Three-Way Catalyst on Gaseous and Particulate Matter Emissions During Gasoline Direct Injection Engine Cold-start

Analysing emissions to meet Euro 6c legislation

Maria Bogarra, Jose Martin Herreros, Cruz Hergueta, Athanasios Tsolakis*
Mechanical Engineering, University of Birmingham, Edgbaston, B15 2TT, UK

***Email:** a.tsolakis@bham.ac.uk

Andrew P. E. York and Paul J. Millington
Johnson Matthey, Blount's Court, Sonning Common, Reading, RG4 9NH, UK

The development of gasoline direct injection (GDI) engines has provided a strong alternative to port fuel injection engines as they offer increased power output and better fuel economy and carbon dioxide emissions. However, particulate matter (PM) emission reduction from GDI still remains a challenge that needs to be addressed in order to fulfil the increasingly stricter environmental regulations. A large number of the total particulate emissions during driving cycles are produced during the engine cold-start. Therefore, controlling PM during cold-start events will significantly reduce the final PM output.

This research work provides an understanding of PM characterisation from a 2 l four-cylinder GDI engine during cold-start. Gaseous emissions including hydrocarbon (HC) speciation studies are also carried out pre- and post- a Euro 6 compliant three-way catalyst (TWC). In addition, particulate size distribution and total particulate number were recorded for the first 280 seconds after the engine cold-start. Large concentrations of carbon monoxide, propane, acetaldehyde, formaldehyde, ethanol, toluene and ethylene were emitted during the first 70–90 seconds from the engine start. Gaseous emissions were reduced on the catalyst at temperatures higher than 290°C, with the catalyst reaching almost 100% removal efficiency at 350°C. The effect of the TWC on PM emissions has been analysed for the different PM diameter ranges. A reduction of particles smaller than 20 nm was observed as well as a reduction in the accumulation mode. In order to understand the nature of the particles emitted during cold-start, transmission electron microscope (TEM) grids were used for particulate collection at the engine start and after 80 seconds and 140 seconds of engine operation. A peak of 1.4×10^8 particles was produced at the engine start and this steadily reduced to 3×10^7 in 50 seconds. The TEM micrographs showed solid particles with similar fractal-like shapes.

1. Introduction

The fleet of GDI engines will continuously increase for years to come due to their significant advantages in terms of fuel consumption and CO_2 reduction when compared to older port fuel injection engines, and the negative publicity diesel vehicles are receiving (1–3). However, GDI engines have been associated with an increase in PM levels when compared to earlier gasoline powertrains. Euro 6c emission legislation limits the number to 6×10^{11} particles km^{-1} and came into force in September 2017 (4). The

main contributor to the total particulate number is small particles (i.e. those formed in the nucleation mode), which are more hazardous to human health than larger particles as they are able to penetrate deeper into the human respiratory system (5). Due to the difficulties when measuring the nucleation mode, the Particle Measurement Programme (PMP) established the cut-off to be 23 nm particles in order to assure the repeatability of the results (6). However, sub-23 nm particles have been reported during GDI normal operation (7, 8) and particles around 6 nm diameter have been found using TEM (9). The high variability of cold-start events, as well as the low temperature in the exhaust and TWC, hinders the measurement of PM. In addition, during the engine cold-start a large amount of fuel is being injected and this increases the emission of larger particles (10). During urban journeys, the engine is subjected to several cold-starts. Although the engine can be warmed, the low exhaust temperature reduces the effectiveness of the aftertreatment system as well as increasing the likelihood of nucleation and the formation of small particles in the exhaust. Engine cold-starts represent 50% of urban driving emissions and contribute to 80% of the total emissions for some species such as volatile organic compounds (11). The emission of unburnt HC during engine cold-start is also an area of concern. Amongst the species found during the engine start is methane, a potent greenhouse gas with radiation trapping efficiency of approximately 25 times higher than CO_2 (12), while polyaromatic HC such as benzene and toluene are carcinogenic to humans (13). This is particularly worrying as in urban areas human exposure is high. Cold-starts are estimated to last for 120 seconds, which is equivalent to a one-mile journey (11). Although the TWC is an efficient way of removing CO, unburned HCs and nitrogen oxides (NOx) from the exhaust, during cold-starts its temperature is far from the ideal operating conditions, reducing the TWC's efficiency. In addition, as PM control is not the main objective of the TWC, its effect on PM during cold-starts is not yet well documented.

Peckham *et al.* (14) studied the legislated emissions using fast-response analysers during the first 100 seconds of the engine cold-start. Approximately 0.31 g of HC, 0.08 g of NOx and almost 2 g of CO were emitted during this period. The main contribution to the cumulative tailpipe emissions were the first 20 seconds of the cold-start, during which several particulate number spikes were emitted. The TWC was reported to reduce the aggressive spikes of the HCs and NOx produced during the cold-start even if the catalyst temperature was still low, although the CO reduction was less noticeable. The TWC reached 300°C after 21 seconds of operation. The same authors in a different study compared the raw engine emissions during cold-start with the results obtained using a PMP compliant dilution tunnel (cut-off of 23 nm) (15). The difference between raw and PMP results are more than one order of magnitude. Rich conditions during cold-start led to several peaks in PM number. The presence of two differentiated PM modes, nucleation and accumulation, during the cold-start suggested the coexistence of particles formed under different conditions in the combustion chamber. Samuel *et al.* (16) analysed the performance of the TWC on PM reduction during cold-start. According to their results, particles between 5 to 25 nm represented 99% of the total emissions until the engine was warmed-up. The TWC was capable of reducing the number of particles emitted, especially those ranging between 5–25 nm and 50–100 nm. The effect of the TWC on particulate size distribution at steady-state condition has been analysed (17). A reduction in the particle concentration around 5–50 nm after the catalytic converter was reported. However, particles above 100 nm were increased. The authors claim that the TWC is able to remove and oxidise some of the PM, but particles may coagulate in the catalyst increasing the diameter of particles post-TWC. Soot oxidation behaviour, nanostructure and Raman analysis during cold-start was analysed (18). The authors reported higher reactivity of the particles collected during the engine cold-start with respect to hot steady-state soot samples. This effect was attributed to the high percentage of unburned ash precursors found in cold-start soot samples. The nanostructure and Raman analysis also showed that during cold-start the soot had an ordered structure similar to warm steady-state conditions meaning that the carbon crystalline structures during cold-start are similar to those during steady-state operation.

In this research, gaseous emissions including HC speciation and PM characterisation during engine cold-start have been measured on an air-guided 2 l four-cylinder GDI engine equipped with a Euro 6 compliant TWC. In addition, total particulate number was recorded in the first 280 seconds of the engine cold-start. The particle size distribution and the fraction of particles per diameter have been analysed at different stages during the engine start (cold-start and after 80 and 140 seconds of engine

operation). Additional PM characterisation studies were carried out using TEM. PM was collected from the engine exhaust gas at different time intervals using copper grids and analysed by TEM in order to understand qualitatively their morphology.

2. Experimental Setup and Method

2.1 Experimental Setup

The engine used for this study was a 2 l, four-cylinder, air-guided stoichiometric GDI. The details of the engine specification can be found in **Table I**. Standard EN228 gasoline with 5% (v/v) ethanol content provided by Shell was used for this research. Fuel properties are presented in **Table II**. 5W30 fully synthetic lubricating oil was employed.

Gaseous emissions were measured using a Fourier-transform infrared spectroscopy (FTIR) 2100 MKS. Legislated emissions (CO, CO_2, NOx and total HC (THC)) as well as HC speciation were sampled before and after the TWC during the cold-start. The sample was filtered to avoid any damage of the optical part by PM and pumped at a rate of 1 l min^{-1} through the equipment. The heating lines and the pump were maintained at 191°C to eliminate any condensation of HCs and water in the pipes.

Total particulate number and size distributions were obtained using a Dekati Electrical Low Pressure Impactor (ELPI®+). An ejector diluter system was used to precondition the sample. The dilution ratio (DR) was set at 10 and recorded throughout the test based on nitric oxide (NO) and CO_2 concentration on the exhaust and diluted streams, Equation (i), using the FTIR. The air dilution temperature was ambient.

$$DR = \frac{ppmNO_{raw\ exhaust}}{ppmNO_{dilute\ sample}} \approx \frac{\%CO_{2\ raw\ exhaust}}{\%CO_{2\ dilute\ sample}} \quad (i)$$

Table I Engine Specifications

Compression ratio	10:1
Bore × stroke	87.5 × 83.1 mm
Turbocharger	Borg Warner K03
Rated power	149 kW at 6000 rpm
Rated torque	300 Nm at 1750–4500 rpm
Engine management	Bosch Me17

Table II Gasoline Properties

Analysis (test method)	Result
Density at 15°C, kg m^{-3}	743.9
Initial boiling point, °C	34.6
20% v/v, °C	55.8
50% v/v, °C	94.0
Final boiling point, °C	186.3
C m/m, %	84.16
H m/m, %	13.48
O m/m, %	2.36
Paraffins, vol%	43.9
Olefins, vol%	11.7
Naphthenes, vol%	7.8
Aromatics, vol%	26.9
Oxygenates, vol%	7.7
Sulfur, ppm	6
Calorific values, MJ kg^{-1}	42.22
Motor octane number	85.3
Research octane number	96.5

2.2 Test Procedure and Method

All the experiments were carried out at cold-start conditions. At least 24 hours were left between tests to soak the engine. The engine warm-up process was established by the test control system (CADET) following standard vehicle operation, the torque and speed trace during this process is provided in **Figure 1**. In addition, to further understand the behaviour of gaseous and PM emissions, the lambda trace during this period is also shown in **Figure 2**. The engine starts at 20 seconds, a sudden increase to 1200 rpm and 5 Nm is produced and the overall lambda is rich at this point to start the combustion. High fluctuations in lambda are produced to stabilise the engine. From this point, different changes in speed and torque are programmed to warm-up the engine leading to changes in lambda that affect gaseous and PM emissions. At the end of the sequence, lambda tends to one.

Gaseous and PM emissions were measured during the first 280 seconds after the engine start pre- and post-TWC. The location of the ELPI®+ and the FTIR sampling point pre- and post-TWC was swapped in each test until a total of five measurements

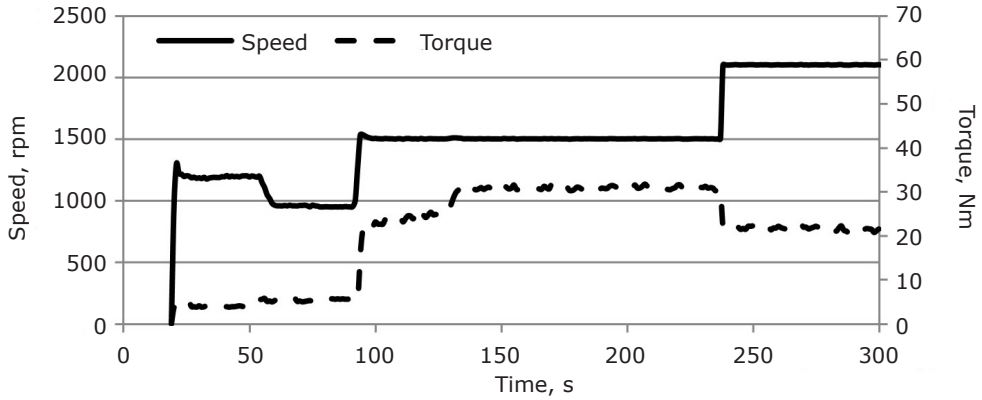

Fig. 1. Torque and speed trace during engine cold-start

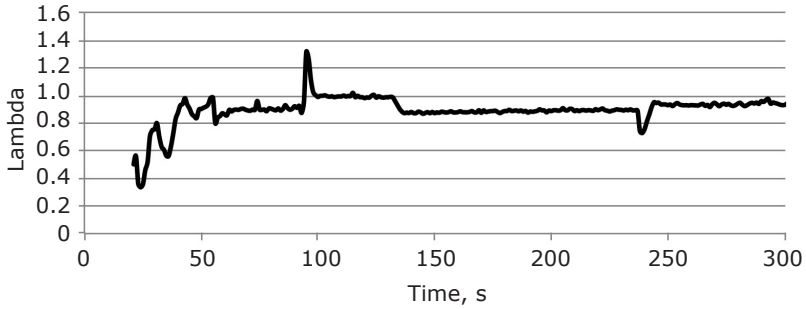

Fig. 2. Lambda trace during engine cold-start

before and after TWC were obtained for statistical analysis. For morphology analysis 3.05 mm, TAAB Formvar coated copper grids were loaded directly from the exhaust pipe at the engine start and after 80 seconds and 140 seconds of engine operation. A schematic of the experimental setup is provided in **Figure 3**.

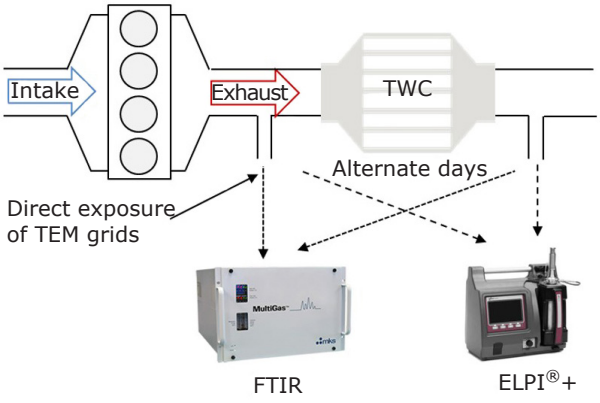

Fig. 3. Experimental setup for measuring emissions during engine cold-start in the present study

3. Results and Discussion

3.1 Gaseous Emissions

3.1.1 Regulated Emissions

The regulated gaseous emissions measured in the engine exhaust before and after the TWC in the first 280 seconds are presented in **Figure 4**. No apparent changes in the gas composition pre- and post-catalyst can be observed in the first 150 seconds. A peak of CO of 10,000 ppm is produced just after the engine start, corresponding to overall rich lambda conditions and this is rapidly decreased to around 1300 ppm. At 235 seconds, engine acceleration leads to an increase in CO. On the other hand, HC emissions remained stable at 4000 ppm during this cold-start period, therefore HC emissions are not influenced by the engine conditions. No oxidation of CO and THC was observed during the first 120 seconds of the engine operation. At this point the exhaust pre-TWC reached temperatures higher than 300°C and the oxidation of HC and CO started. NO reduction did not start until the TWC temperature exceeded 300°C.

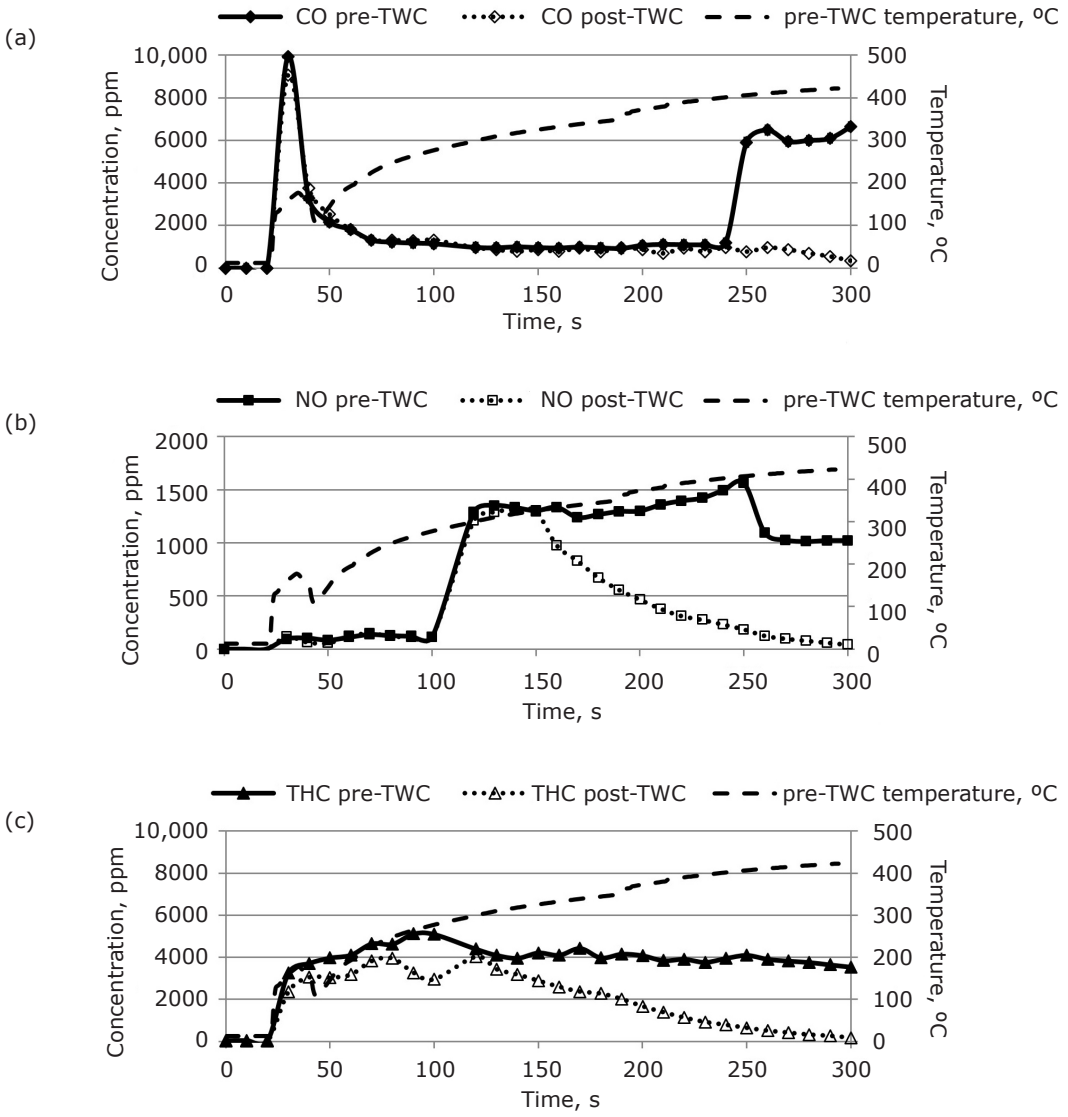

Fig. 4. Emissions during cold-start: (a) CO; (b) NOx; (c) THC

3.1.2 Hydrocarbon Speciation

The different HC species measured by the FTIR are divided in three groups:

(a) linear HC species (**Figure 5(a)**)
(b) oxygenated HCs (**Figure 5(b)**)
(c) unsaturated HCs (**Figure 5(c)**).

The reactivity of individual HC species is affected by the exhaust composition. In addition, CO oxidation and NO reduction are affected by the different HC present in the exhaust and the intermediate species formed on the catalyst during HC oxidation, such as ethoxide, acetate, formate and benzoate (19). For instance the higher reactivity of the HC will lead to an increased inhibition of CO oxidation due to the competition for active sites (20). On the other hand, unsaturated species are beneficial for NO reduction (19). During the cold-start analysed in this work, the most abundant species are light HC such as propane, acetaldehyde, formaldehyde, acetylene and ethylene. The TWC is not able to effectively remove these species during the first 200 seconds due to the low temperature. From this point, the catalyst is closer to its light-off temperature, reducing all HC species, and reached 100% conversion at approximately 230 seconds after engine start. The HC reactivity follows the order reported in the literature: alcohols > aldehydes > aromatics > alkenes > alkanes (21).

Linear HCs: more than 600 ppm of propane were observed pre-TWC, **Figure 5(a)**. The concentration after TWC fluctuated before the catalyst temperature

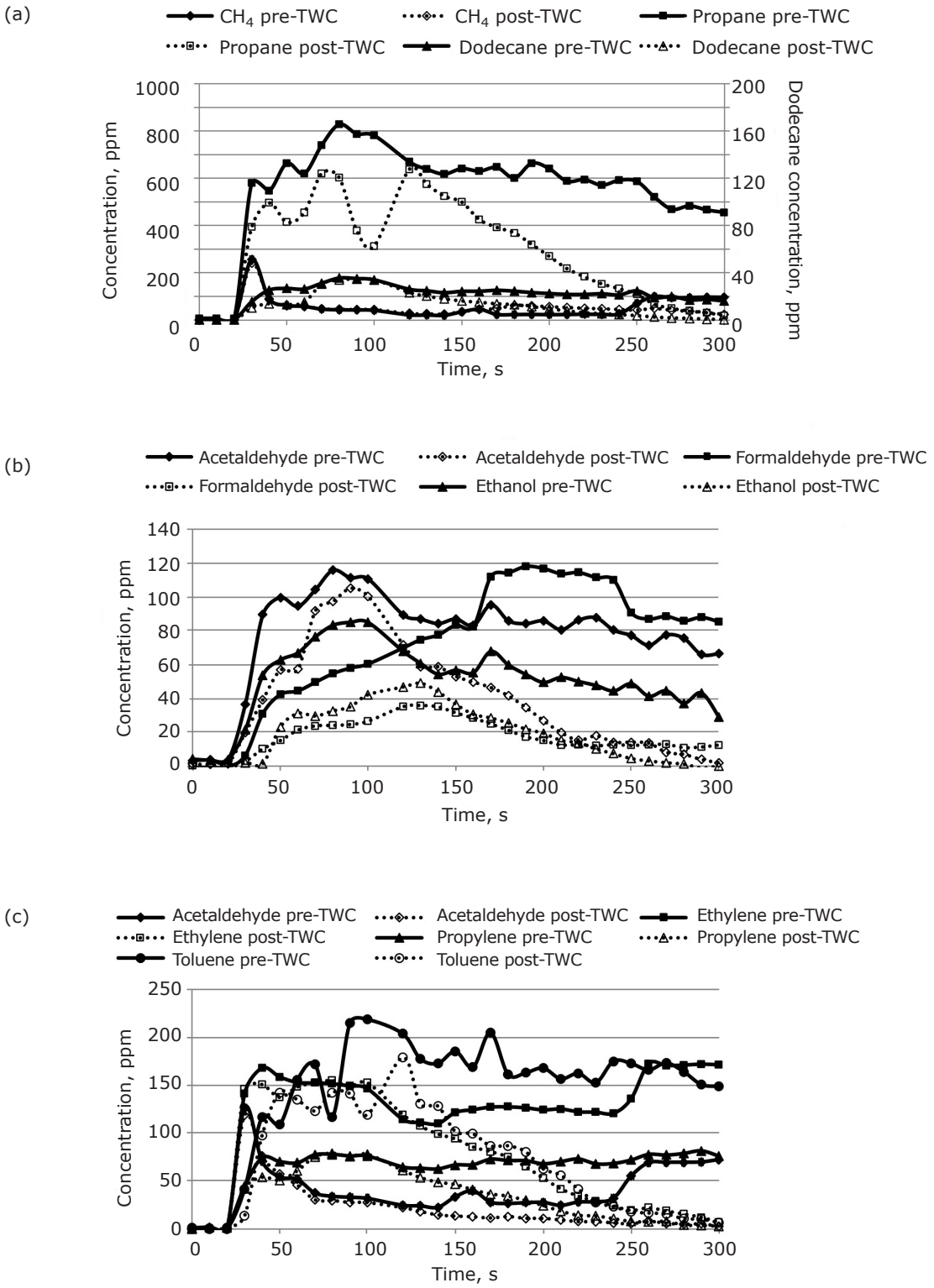

Fig. 5. HC speciation during cold-start: pre-TWC and post-TWC: (a) linear HCs; (b) oxygenated HCs; (c) unsaturated HCs

reached 300°C. At this point the propane concentration decreased steadily until reaching negligible engine-out concentration at 420°C, 250 seconds after the engine start. The second highest engine output emission concentration was methane: 220 ppm were produced just after the engine start but as the engine warmed up the engine output concentration was then rapidly reduced and stabilised at around 50 ppm. The pre- and post-TWC methane concentration was similar for the entire study and no oxidation activity was observed. Methane emissions are a major concern

due to its global warming potential, its link with ozone formation (12) and the difficulty of oxidising methane in the TWC (22). The oxidation of the approximately 20 ppm of dodecane was observed earlier than propane. The longer the alkane chain, the lower the light-off temperature required (19).

Oxygenated HCs: the largest concentration of measured oxygenated species emitted was acetaldehyde, followed by ethanol and then formaldehyde, **Figure 5(b)**. The formation of acetaldehyde and formaldehyde, unregulated compounds classified as carcinogenic to humans, has been reported during the incomplete combustion of ethanol blends (23, 24). More than 100 ppm of acetaldehyde were produced during the engine start, and the start of oxidation was observed at a temperature of 280°C, earlier than NO, CO and the rest of the HC species. The maximum concentration of formaldehyde emissions during the first 70 seconds of the engine operation was around 60 ppm. The TWC seemed to store part of the acetaldehyde and formaldehyde until the catalyst was close to its light-off temperature (350°C). The condensation of HC on the TWC during cold-start due to the cold catalyst surface is linked with a delay in CO conversion (20). The light-off activity for formaldehyde is similar to that of acetaldehyde. Aldehydes have been reported to be more reactive than aromatics and alkanes (21). However, ethanol emissions reached 80 ppm and started decreasing at 300°C. Ethanol light-off temperature has been reported to be lower than that of CO, despite the higher C–H bonding energy when compared to propane or toluene. The dipole-dipole interaction of the polar ethanol molecule's functional group with the surface of the catalyst is the reason for the higher oxidation activity of ethanol (19).

Unsaturated HCs: toluene and ethylene are the two main unsaturated HC species emitted from the engine, **Figure 5(c)**. At the engine start, a peak of 160 ppm of ethylene was produced. After 100 seconds of engine operation the ethylene concentration started declining steadily, reaching close to 0 ppm after 230 seconds. Ethylene and propylene are more reactive than alkane species and adsorb more easily on the catalyst surface leading to earlier light-off (20). The toluene peak was delayed with respect to the other species and a maximum concentration of 250 ppm was observed after 70 seconds from the engine start. At this point and similarly to ethylene's behaviour, the concentration decreased almost linearly. Acetylene peaked at 125 ppm at the cold-start and showed stronger adsorption behaviour than ethylene or propylene; this can lead to CO oxidation inhibition (20).

3.2 Particulate Matter

3.2.1 Particle Number During Cold-start

The evolution of PM during the first few seconds of the engine cold-start is presented in **Figure 6**, note that scales pre- and post-TWC are different. A significant peak of particles, 1.3×10^8 particles cm^{-3}, was initially recorded before its rapid reduction during the first 70 seconds. These high PM levels correspond to overall rich lambdas. As

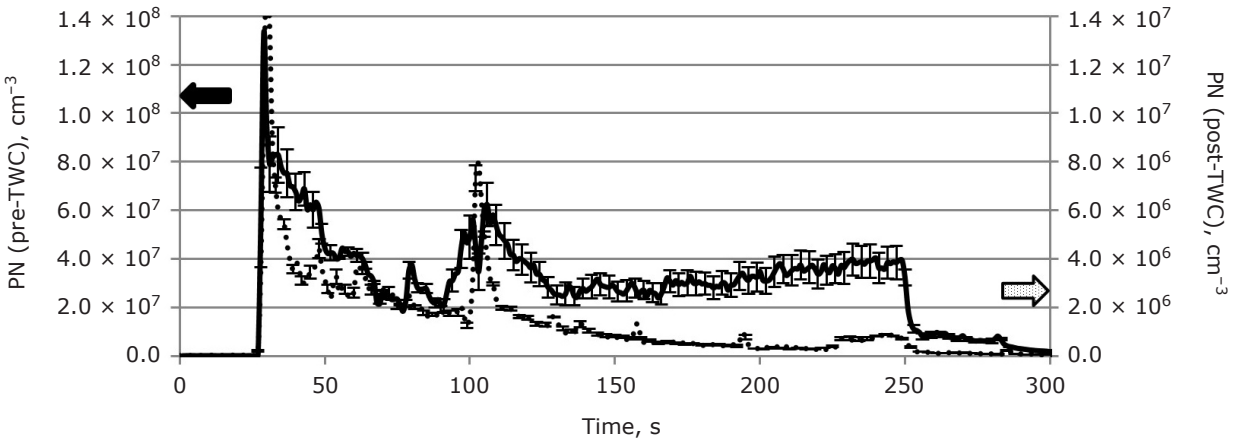

Fig. 6. Particle number emissions during engine cold-start. Effect of the TWC. Note that scales pre- and post-TWC are different

in the case of CO engine output emissions, at this stage PM levels are highly influenced by lambda fluctuations. The TWC is able to considerably reduce the amount of PM emitted even though at this early stage it is far from its light-off temperature. Particle losses in catalysts have been mainly attributed to particle diffusion and thermophoresis (25). Particle removal by diffusion is significant for particles below 100 nm. At 10 nm 75% of the particles have been reported to be reduced in a catalyst by diffusion (25). In addition thermophoretic losses during transient operation can be around 20% (26). These results suggest that PM formed by heavy HCs are condensed in the TWC on account of the temperature conditions and can either (a) be oxidised or (b) blow-off the TWC when the temperature reaches the light-off conditions. In addition, FTIR is only able to measure some light HC species in the gas-phase suggesting that PM are composed by a soot core and heavier polyaromatic HCs. The need for enrichment to assure the engine cold-start, worsened by piston and wall-impingement of the fuel, leads to the formation of fuel-rich areas promoting PM formation (27).

3.2.2 Particulate Size Distributions and Diameter Fractions During Cold-Start

The particulate size distributions before and after the TWC at the engine start and after 80 seconds and 140 seconds of engine operation are presented in **Figures 7–9**, note that scales pre- and post-TWC are different. TEM images before the TWC have been included as well for qualitative analysis of soot pre-TWC. All the distributions showed a bimodal shape with nucleation particles smaller than 20 nm and an accumulation mode centred between 50–100 nm. At the engine start the accumulation mode measured pre-TWC was centred at 70 nm. The catalyst was capable of storing and trapping small particles and HC droplets as well as reducing the accumulation mode, leading to a shift in the peak to 30 nm. On the other hand, after 80 and 140 seconds of engine operation, the TWC was capable of eliminating particles smaller than 20 nm and larger than 50 nm without affecting particles in the range 20–50 nm. This lack of effect between 20–50 nm has been previously reported in the literature (16). Larger particles (accumulation peak centred in 120 nm) were observed pre-TWC.

At first glance, the TEM grids corresponding to the first stage of the cold-start were heavily loaded, (**Figure 7(b)**) and had a fractal-like appearance similar to GDI engine steady-state operation or even similar to diesel. The majority of the particles collected in the grid pre-TWC for the TEM analysis were solid, a result that has previously been observed (15). Different types of particles were found pre-TWC, fractal-like agglomerates similar to diesel particles (**Figure 8(b)** or **Figures 7(b)** and **7(c)**) and slurry-like particles (**Figure 8(c)**). Furthermore, the presence of small spherules (**Figure 7(c)**) was also observed. The presence of different types of PM has been previously reported in the literature (9, 28). After 80 seconds, the concentration of particles found in the grid dropped significantly. At this point the engine decelerated, leading to an increase in the air fraction. Lambda was still rich but approximating to stoichiometric conditions; still the four types of PM aforementioned were observed. At 140 seconds after the engine start, only a few solid particles were found under the TEM beam. Although the engine accelerated, the air-fuel mixture may be already homogeneous reducing the overall formation of particles. It is well-known that the main contributor to PM emissions in GDI engines is cold-start and transient operation. It has been suggested that the nature of this PM was volatile HC; however, the images clearly show the presence of soot at this early stage of the engine operation in agreement with where solid particles have previously been found (18).

Figure 10 presents the percentage of particles in each of the measured diameter ranges before and after the TWC. Sub-23 nm particles account for up to 67% of total PM emitted. The TWC considerably reduced the amount of particles between 5–10 nm, however, up to 40% of sub-23 nm particles were observed at 140 seconds after engine start (**Figure 10(b)**). The origin of sub-23 nm particles in GDI engines is thought to be metals from the lubricant oil or from the fuel additives. The percentage of solid sub-23 nm is typically below 60%, similar to the results obtained in this work, slightly exceeding the sub-23 nm fraction reported for diesel engines (29). The results show that the TWC itself can have a reducing effect on the PM, but that an additional catalyst system will be required for full PM control; this will be in the form of a particulate filter.

4. Conclusions

Gaseous emissions, HC species and PM have been analysed during cold-start engine conditions for the first 280 seconds after engine start. The performance of a Euro 6c compliant TWC in gaseous

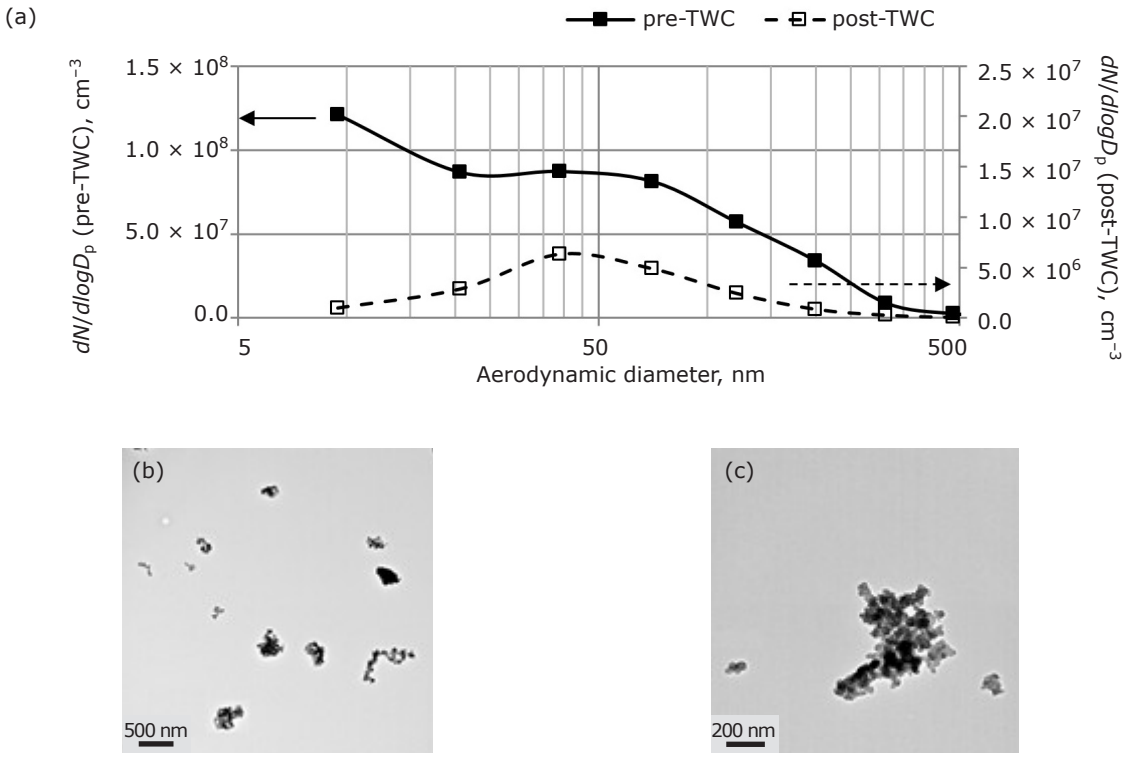

Fig. 7. Engine start: (a) particulate size distribution (PSD); (b) TEM micrograph; (c) TEM micrograph showing particles with a different nature. Note that scales pre- and post-TWC are different

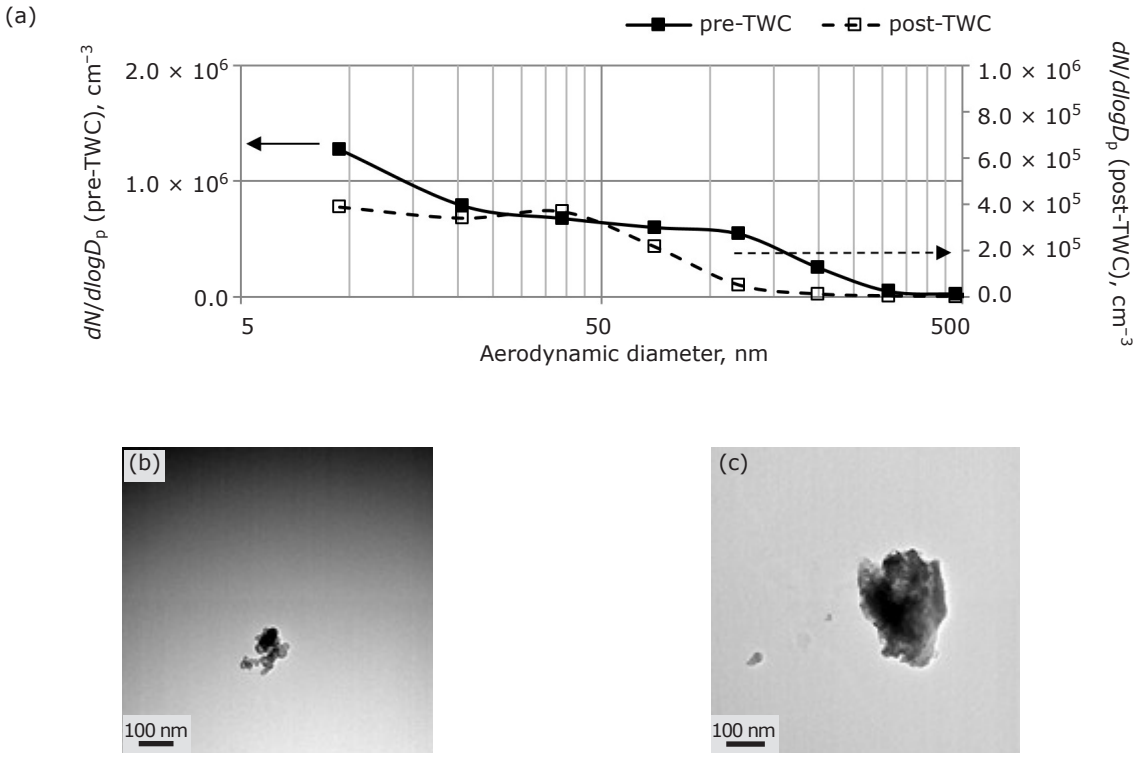

Fig. 8. 80 seconds of engine operation: (a) PSD; (b) TEM micrograph; (c) TEM micrograph showing particles with a different nature. Note that scales pre- and post-TWC are different

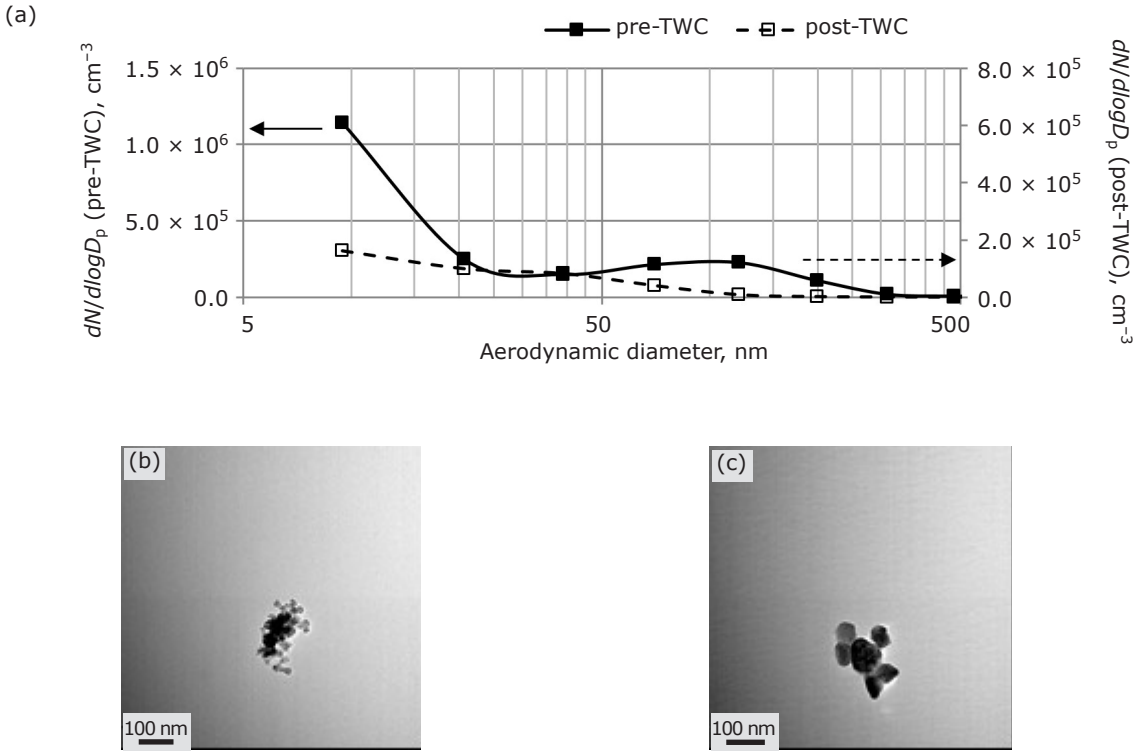

Fig. 9. 140 seconds of engine operation: (a) PSD; (b) TEM micrograph; (c) TEM micrograph showing particles with a different nature. Note that scales pre- and post-TWC are different

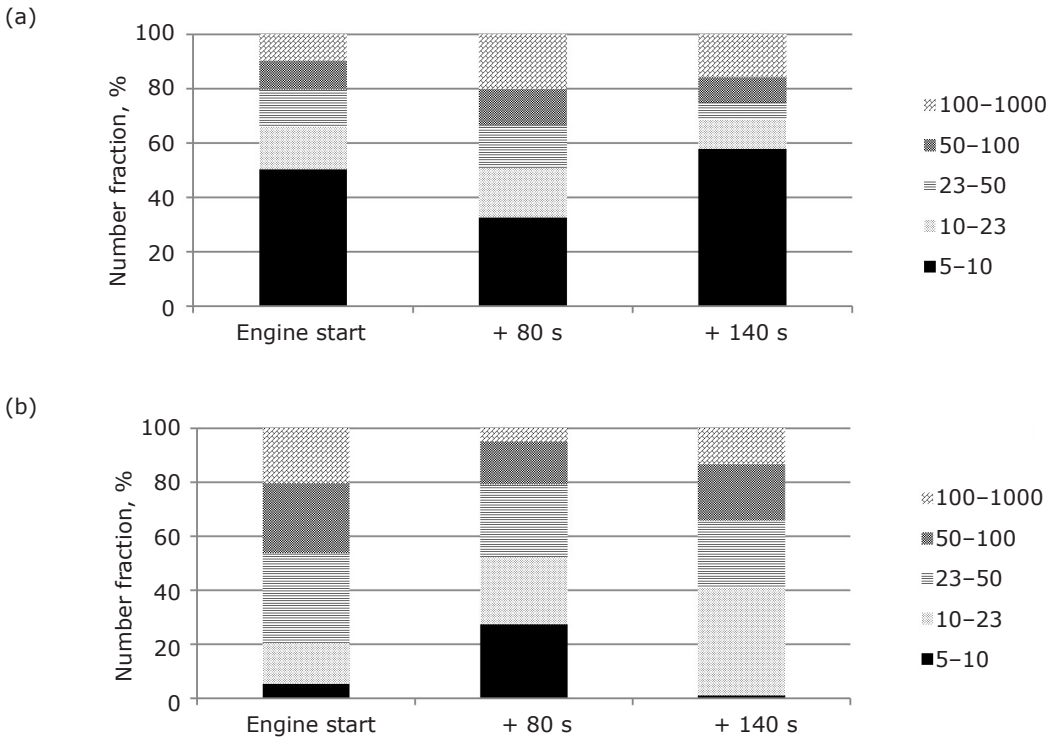

Fig. 10. Percentage fraction of particles per diameter: (a) pre-TWC; (b) post-TWC

emissions removal during this period has been assessed as well as its effect on PM emissions.

The TWC effectively reduced NO, CO and THC for temperatures above 300°C. However, before the catalyst light-off, large quantities of methane, propane, toluene, ethanol, acetaldehyde and formaldehyde were emitted. The HC reactivity followed the order: alcohols > aldehydes > aromatics > alkenes > alkanes during the period analysed.

Total particle number emissions peaked at 1.4×10^8 particles cm^{-3} at the engine start and dropped an order of magnitude after 140 seconds of the engine warming up. A significant concentration of sub-23 nm was observed pre-TWC. HC and particle deposition on the TWC have been observed during the cold-start which can delay CO oxidation. Particle size distributions showed a bimodal distribution along the 280 seconds of the analysis. The TWC was able to reduce the number of particles between 5–10 nm, but still a significant concentration of particles between 10–23 nm was observed. The particles observed during the engine cold-start are solid and fractal-like similar to diesel PM.

Acknowledgments

The authors would like to thank EPSRC and Johnson Matthey for funding the project and providing a scholarship to Maria Bogarra. Innovate UK (Technology Strategy Board) is acknowledged for supporting this work with the project "CO_2 Reduction through Emissions Optimisation" (CREO: ref. 400176/149) in collaboration with Ford Motor Company, UK; Jaguar Land Rover, UK, and Cambustion, UK. The Advantage West Midlands and the European Regional Development Fund as part of the Science City Research Alliance Energy Efficiency Project are also acknowledged for supporting the research work. Louie Chen from Scielutions Ltd, UK, and Dekati Ltd, Finland, are also acknowledged for the use of the ELPI®+.

Glossary Terms

CO	carbon monoxide
CO_2	carbon dioxide
DR	dilution ratio
ELPI®+	electrical low pressure impactor
FTIR	Fourier transform infrared
GDI	gasoline direct injection engine
HC	hydrocarbon
NOx	nitrogen oxides
PM	particulate matter
PMP	particle measurement programme
PSD	particulate size distribution
SMPS	scanning mobility particulate sizer
TEM	transmission electron microscope
TWC	three-way catalyst
VOC	volatile organic compound

References

1. "Advanced Direct Injection Combustion Engine Technologies and Development: Gasoline and Gas Engines", 1st Edn., ed. H. Zhao, Vol. 1, Woodhead Publishing Ltd, Cambridge, UK, 2010, pp. 1–19
2. V. Franco, F. P. Sánchez, J. German and P. Mock, "Real-World Exhaust Emissions from Modern Diesel Cars: A Meta-Analysis of PEMS Emissions Data from EU (Euro 6) and US (Tier 2 Bin 5/ULEV II) Diesel Passenger Cars: Part 1: Aggregated Results", The International Council of Clean Transportation, Berlin, Germany, 2014
3. "European Vehicle Market Statistics: Pocketbook 2016/17", ed. P. Mock, The International Council of Clean Transportation, Berlin, Germany, 2016
4. Commission Regulation (EU) 459/2012, *Official J. Eur. Union*, 2012, **55**, (L142), 16
5. K.-H. Kim, E. Kabir and S. Kabir, *Environ. Int.*, 2015, **74**, 136
6. B. Giechaskiel, R. Chirico, P. F. DeCarlo, M. Clairotte, T. Adam, G. Martini, M. F. Heringa, R. Richter, A. S. H. Prevot, U. Baltensperger and C. Astorga, *Sci. Total Environ.*, 2010, **408**, (21), 5106
7. I. Khalek, T. Bougher and J. Jetter, *SAE Int. J. Fuels Lubr.*, 2010, **3**, (2), 623
8. T. Rönkkö, L. Pirjola, L. Ntziachristos, J. Heikkilä, P. Karjalainen, R. Hillamo and J. Keskinen, *Environ. Sci. Technol.*, 2014, **48**, (3), 2043
9. T. L. Barone, J. M. E. Storey, A. D. Youngquist and J. P. Szybist, *Atmos. Environ.*, 2012, **49**, 268
10. C. K. Gaddam and R. L. Vander Wal, *Combust. Flame*, 2013, **160**, (11), 2517
11. M. S. Reiter and K. M. Kockelman, *Transport. Res. D: Transport Environ.*, 2016, **43**, 123
12. "Inventory of U.S. Greenhouse Gas Emissions and Sinks: 1990–2015", EPA 430-P-17-001, US Environmental Protection Agency, Washington, DC, USA, 13th April, 2017, 633 pp
13. A. J. McMichael, 'Carcinogenicity of Benzene, Toluene and Xylene: Epidemiological and Experimental Evidence' in "Environmental Carcinogens: Methods of Analysis and Exposure Measurement: Benzene and Alkylated Benzenes", eds. L. Fishbein and I. K. O'Neill, IARC Scientific Publications No. 85, Vol. 10, International Agency for Research on Cancer, Lyon, France, 1988, pp. 3–18

14. M. S. Peckham, A. Finch and B. Campbell, *SAE Int. J. Engines*, 2011, **4**, (1), 1513
15. M. S. Peckham, A. Finch, B. Campbell, P. Price and M. T. Davies, 'Study of Particle Number Emissions from a Turbocharged Gasoline Direct Injection (GDI) Engine Including Data from a Fast-Response Particle Size Spectrometer', SAE Technical Paper 2011-01-1224, 2011
16. S. Samuel, A. Hassaneen and D. Morrey, 'Particulate Matter Emissions and the Role of Catalytic Converter During Cold Start of GDI Engine', SAE Technical Paper 2010-01-2122, 2010
17. I. Whelan, S. Samuel and A. Hassaneen, 'Investigation into the Role of Catalytic Converters on Tailpipe-Out Nano-Scale Particulate Matter from Gasoline Direct Injection Engine', SAE Technical Paper 2010-01-1572, 5th May, 2010
18. S. Choi and H. Seong, *Combust. Flame*, 2015, **162**, (6), 2371
19. S. B. Kang, S. B. Nam, B. K. Cho, I.-S. Nam, C. H. Kim and S. H. Oh, *Catal. Today*, 2014, **231**, 3
20. T. Bäroth, A. Drochner, H. Vogel and M. Votsmeier, *Top. Catal*., 2017, **60**, (3–5), 278
21. A. O. Rusu and E. Dumitriu, *Environ. Eng. Manage. J*., 2003, **2**, (4), 273
22. G. Beulertz, M. Votsmeier and R. Moos, *Appl. Catal. B: Environ.*, 2015, **165**, 369
23. R. Suarez-Bertoa, A. A. Zardini, H. Keuken and C. Astorga, *Fuel*, 2015, **143**, 173
24. S. Paz-Estivill, R. Delgado-Ortiz, E. Cirera-Domènech and F. Broto-Puig, 'Vehicle Exhaust Emissions Characterization by Chromatographic Techniques Applied to Different Gasoline-Ethanol Blends', SAE Technical Paper 2013-01-1044, 2013
25. J. Swanson, W. Watts, D. Kittelson, R. Newman and R. Ziebarth, *Aerosol Sci. Technol*., 2013, **47**, (4), 452
26. J. E. Johnson and D. B. Kittelson, *Appl. Catal. B: Environ.,* 1996, **10**, (1–3), 117
27. H. Badshah, D. Kittelson and W. Northrop, *SAE Int. J. Engines*, 2016, **9**, (3), 1775
28. P. Karjalainen, L. Pirjola, J. Heikkilä, T. Lähde, T. Tzamkiozis, L. Ntziachristos, J. Keskinen and T. Rönkkö, *Atmos. Environ*., 2014, **97**, 262
29. B. Giechaskiel and G. Martini, 'PMP: SUB 23 NM Review', UNECE, Particle Measurement Programme (PMP), 28th Session, Brussels, Belgium, 21st November, 2013

The Authors

Maria Bogarra is a Research Fellow working on a Horizon 2020 funded project at the School of Engineering, University of Birmingham, UK. She obtained her PhD degree in Mechanical Engineering entitled "Characterisation of Particulate Matter Emitted by Gasoline Direct Injection Engines" at the University of Birmingham in March 2017. She has worked in the physical-chemical characterisation of alternative fuels, the performance of aftertreatment systems and alternative fuels for both diesel and gasoline powertrains and on the development of methods for the characterisation of particulate matter emitted by gasoline direct injection engines.

Dr Jose M. Herreros is a Lecturer in Vehicle Engineering at the School of Engineering at the University of Birmingham. His research focuses on the investigation of clean and efficient powertrain systems based on the energy and emissions efficient integration of various propulsion systems with the ultimate goal to develop energy-efficient and clean powertrains to be used in vehicular applications. He has published journal articles on issues related to fuel design and properties, pollutant emissions characterisation and catalysis.

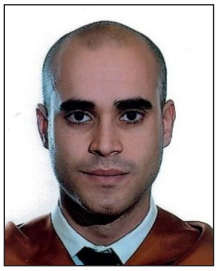

Cruz Hergueta Santos-Olmo studied Mechanical Engineering at University of Castilla-La Mancha (UCLM), Spain, between 2007 and 2012. In September 2015 he was successful with his scholarship application to fund his PhD studies and since then he is a Doctoral Candidate at the Department of Mechanical Engineering at the University of Birmingham. The research work is focused on gasoline-bio-alcohols blends (gasoline-ethanol and gasoline-butanol) performance on modern gasoline direct injection engines combined with alternative technological solutions such as exhaust gas recirculation strategies, reformed exhaust gas recirculation and gasoline particulate filters for improving efficiency and emissions reduction.

Professor Athanasios Tsolakis has academic and industrial expertise in the field of low carbon energy carriers, environmental catalysts, combustion and pollutant control technologies. He works at the forefront of basic and translational research to improve fuel efficiency and reduce the environmental impact of the transportation and power generation sectors. Prior to his academic appointment at the University of Birmingham in 2005 he worked as a research scientist at Johnson Matthey in the design and characterisation of environmental catalysts for modern aftertreatment systems. Professor Tsolakis has successfully supervised to completion 27 doctoral researchers. In 2009 he was elected Fellow of the Institution of Mechanical Engineers (FIMechE) and in 2011 he was elected Fellow of the Higher Education Academy (FHEA). In 2014 he led the Research Excellence Framework 2014 (REF2014) for the School of Mechanical Engineering and was appointed the Director of Research and Knowledge Transfer for the School. Since 2015 he is the Director of Research for the School of Engineering.

Dr Andy York joined Johnson Matthey, Sonning Common, in 2000 in the Emission Control Research group. He has worked in a variety of roles, including gasoline and diesel catalyst research, and reaction engineering modelling and reaction kinetics. He has also led a collaboration with the University of Cambridge, UK, working on a wide range of academic and business related projects involving catalysis and engineering.

Dr Paul Millington originally joined Johnson Matthey in the Emission Control Research group in 1995. After a short break in the automotive industry he rejoined in 2001. He currently works on all forms of pgm-containing aftertreatment in the Emission Control Research group at Johnson Matthey.